

Spatial Deconvolution Studies of Nearside Lunar Prospector Thorium Abundances. D. J. Lawrence¹, R. C. Elphic¹, W. C. Feldman¹, J. J. Hagerty¹, and T. H. Prettyman¹; ¹Los Alamos National Laboratory, Los Alamos, NM, USA (djlawrence@lanl.gov)

Introduction: Orbital gamma-ray and neutron spectroscopy measurements have greatly contributed to our understanding of the elemental composition of the both the Moon and Mars [1,2,3,4,5]. One drawback, however, to these measurements is that the spatial resolution is quite broad since it is roughly equal to or greater than the spacecraft height above the planetary surface. For example, for the 30-km low altitude Lunar Prospector measurements, the spatial resolution is ~45 km. For the Mars Odyssey gamma-ray and neutron measurements, the spatial resolution is ~600 km for an orbital altitude of 400 km.

The technique of spatial deconvolution [6] offers a way to improve the spatial resolution of these measurements if the spatial response function of the instrument is sufficiently well known. Previous studies have carried out spatial deconvolution for lunar and Mars neutron data [7,8,9]. A constant difficulty in utilizing these techniques is clearly determining the difference between true signal and noise that is amplified by the deconvolution process. This difficulty is managed in various ways by the different studies.

Lunar Prospector data provide a unique opportunity to mitigate this difficulty because large datasets exist for two different altitudes – 100 and 30 km – and hence for two different spatial resolutions. In order to better understand the spatial deconvolution process, we can deconvolve high-altitude data and compare it with the measured low-altitude data, which has a spatial resolution a factor of 3 better than the high-altitude data. A comparison between the deconvolved high-altitude data and measured low-altitude data then provides an indication of the types of errors characteristic of the deconvolution process. With this knowledge, one can then carry out a deconvolution of the low-altitude data. For this set of deconvolution studies, we have used the thorium counting rates measured with the LP gamma-ray spectrometer (LP-GRS). The reason for this is two fold: 1) We have well characterized the LP-GRS spatial response function as a function of altitude [1]; and 2) The thorium counting rates have the highest signal-to-noise of all the LP-GRS data.

Deconvolution Algorithm: To carry out the deconvolution, we employ a nonlinear, iterative technique called Jansson's method [6]. For Jansson's method, iterative solutions are obtained using the following:

$$o^{k+1} = o^k + r(o^k)(i - s \otimes o^k),$$

where o^k is the k th iterate of the solution image, i is the original image, s is the spatial response function, and $r(o^k)$ is a function that ensures the solution stays within reasonable bounds. An advantage to Jansson's method is it is very easy to implement. One drawback, however, is that it does not take into account the noise in the data, and thus it can introduce increased noise artifacts. In comparison, other methods that are more difficult to implement [10] reduce the noise in the solution based on the noise in the data.

Deconvolved High-altitude Data: Figure 1 shows the results when Jansson's method is applied to LP-GRS high-altitude thorium data for the nearside region of $-30^\circ < \text{lat} < +30^\circ$ and $-30^\circ < \text{lon} < +30^\circ$. This is a region where there is large contrast in the thorium data and many small area features are easily recognizable. Fig. 1a shows the original high-altitude map; Fig. 1b shows the deconvolved map after 10 iterations; Fig. 1c shows the low-altitude thorium map for comparison. While the match is not perfect, the comparison between Fig. 1b and 1c does show that the deconvolution does reproduce many of the features seen in the low-altitude data. This gives us confidence that there is utility in the deconvolution process, so we have proceeded to the low-altitude data.

Deconvolved Low-altitude Data: Figure 2 shows the results when we have deconvolved the low-altitude thorium data in the same nearside region. Fig. 2a shows the original low-altitude map; Fig. 2b shows the deconvolved map; Fig. 2c shows high spatial resolution iron data derived using Clementine spectral reflectance data [11]. In previous studies, we showed that in many locations (especially many nearside locations), thorium and iron often show strong correlations (either positive or negative correlations) [1]. In the deconvolved map, we notice a number of striking features. First, the thorium counting rate for Copernicus crater ($-20^\circ, +10^\circ$) in the deconvolved, low-altitude maps is significantly lower than in the measured low-altitude map. This is consistent with previous indications that both thorium and iron are quite low in the center of this crater. We also note that the Fra Mauro region ($-20^\circ < \text{lon} < -10^\circ, -10^\circ < \text{lat} < 0^\circ$, arrows in Figs. 2b, 2c), which has previously been identified as having high thorium abundances both with orbital data and samples (e.g., Apollo 14 is located in Fra Mauro), is more clearly delineated in the deconvolved map. In particular, the spatial distribution of high thorium abundances in this region is closely similar to the spatial distribution of lower iron abundances in the same

region. This is consistent with the idea that this region is dominated by a KREEP basalt type of material, which is higher in thorium and lower in iron compared to surrounding mare basalt materials.

Lassell Red Spot: Figure 3 shows an interesting result from the same low-altitude deconvolved map. The Lassell red spot (the low-iron feature in Fig. 3c located at -8° lon, -15° lat, arrow in Fig. 3c) has recently been identified as a location of high thorium abundances using forward modeling techniques [12,13]. With the deconvolved data (Fig. 3b), we see that there appears to be a good confirmation that the Lassell location is indeed enhanced with thorium abundances (note that a lobe of thorium enhancement is co-located with the red spot). With the original, low-altitude data, the correspondence is not as clear. This gives us confidence that deconvolution techniques can provide additional information about the spatial distribution of low-spatial resolution datasets.

Conclusions: With these preliminary studies, we have gained confidence that spatial deconvolution

techniques can be useful in improving interpretations of low-spatial resolution datasets such as the LP-GRS data. However, the dominant concern with these techniques is properly discriminating the difference between noise and signal. Thus, future work includes characterizing the errors introduced with the deconvolution algorithm. In addition, we plan to study other techniques (nonlinear least squares, Pixon, [10]) that show promise in minimizing the noise in the deconvolved maps.

References: [1] Lawrence et al., JGR, 108, 10.1029/2003JE2050, 2003; [2] Feldman et al., JGR, 105, 20347, 2000; [3] Feldman et al., Science, 297, 75, 2002; [4] Boynton et al., Science, 2297, 81, 2002; [5] Prettyman et al., JGR, 109, 10.1029/2003JE2139, 2004; [6] Jansson, Deconvolution of Images and Spectra, Academic Press, 1997; [7] Elphic et al., 36th LPSC, #2297, 2005; [8] Elphic et al., 36th LPSC, #1805, 2005 [9] Prettyman et al., 36th LPSC, #1384, 2005; [10] Puetter et al., Annu. Rev. Astron. Astrophys. 43, 139, 2004; [11] Lucey et al., 105, 20297, 2000; [12] Hagerty et al., 36th LPSC, #1746, 2005; [13] Hagerty et al., JGR, in review, 2005.

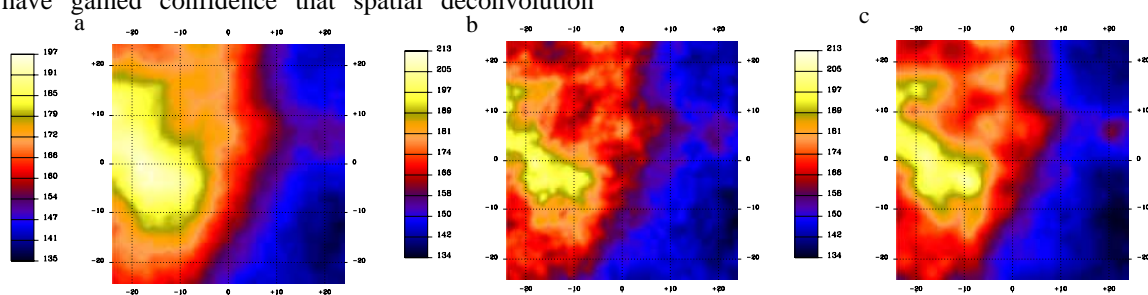


Figure 1. (a) High-altitude nearside thorium abundances; (b) Deconvolved high-altitude thorium abundances; (c) Low-altitude thorium abundances.

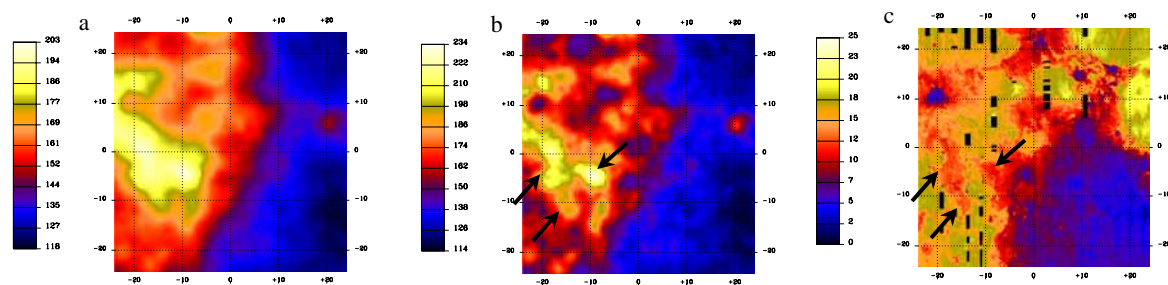


Figure 2. (a) Low-altitude nearside thorium abundances; (b) Deconvolved low-altitude thorium abundances; (c) High spatial resolution iron abundances from Clementine spectral reflectance (CSR) data.

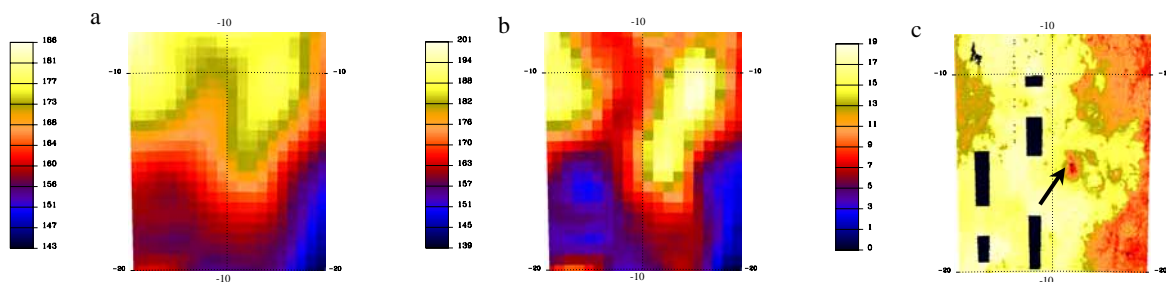


Figure 3. (a) Low-altitude thorium abundances near the Lassell red spot; (b) Deconvolved low-altitude thorium abundances near the Lassell red spot; (c) CSR iron data near the Lassell red spot.